Atmospheric Environment 88 (2014) 83–89

Contents lists available at ScienceDirect

Atmospheric Environment

journal homepage: www.elsevier.com/locate/atmosenv

Characteristics of heavy aerosol pollution during the 2012–2013 winter in Beijing, China

Jiannong Quan [a,b,*], Xuexi Tie [c,d,**], Qiang Zhang [a,b], Quan Liu [a,b], Xia Li [a,b], Yang Gao [a,b], Delong Zhao [a,b]

[a] Beijing Weather Modification Office, Beijing, China
[b] Beijing Key Laboratory of Cloud, Precipitation and Atmospheric Water Resources, Beijing, China
[c] Key Laboratory of Aerosol Science and Technology, SKLLQG, Institute of Earth Environment, Chinese Academy of Sciences, Xian, China
[d] National Center for Atmospheric Research, Boulder, CO, USA

HIGHLIGHTS

- Both aerosol concentrations and RH had strong effect for the occurrence of the haze events.
- The lower PBL height in haze events leads to an increase in the surface aerosol concentrations.
- During the heavy haze events, higher heterogeneous conversions from gas to particle phases of NO_x and SO_2 was observed.

ARTICLE INFO

Article history:
Received 23 October 2013
Received in revised form
21 January 2014
Accepted 24 January 2014
Available online 28 January 2014

Keywords:
Aerosol
Fog and haze
Low visibility
Beijing
PBL height

ABSTRACT

A comprehensive measurement was carried out to analyze the heavy haze events during 2012–2013 winter in Beijing. The measured variables include some important meteorological parameters, such wind directions, wind speeds, relative humidity (RH), planetary boundary layer (PBL), solar radiation, and visibility. The aerosol composition and concentrations (including particular matters ($PM_{2.5}$), nitrate (NO_3), sulfate (SO_4), ammonium (NH_4)) as well as their gas-phase precursors (including nitrogen oxides (NO_x) and sulfur dioxide (SO_2)) were analyzed during the period between Nov. 16, 2012 and Jan. 15, 2013. The results show that the hourly mean concentrations of $PM_{2.5}$ often exceeded 200 μg/m^3, with a maximum concentration of 600 μg/m^3 on Jan. 13, 2013. The relative humidity was increased during the haze events, indicating that both aerosol concentrations and RH had important effect on the reduction of visibility, causing the occurrence of the haze events. Because the wind speeds were generally low (less than 1 m/s) during the haze event, the vertical dispersion and the PBL heights were very important factors for causing the strong variability of aerosol concentrations. This study also finds that under the lower visibility condition, the conversion from the gas-phase of NO_x and SO_2 to the particle phase of NO_3 and SO_4 were higher than the values under the higher visibility condition. Because the lower visibility condition was corresponding to the lower photochemical activity than the higher visibility condition, the higher conversion from gas phase to particle phase in the lower visibility condition indicated that there was important heterogeneous formation of NO_3 and SO_4 during the heavy haze events.

1. Introduction

Beijing is experiencing heavy air pollution in the past two decades, with particle matter (PM) being one of the top pollutants (Chan and Yao, 2008). PM, especially fine particles ($PM_{2.5}$; particle matter with the radius equal/less 2.5 μm) often exceed the new National Ambient Air Quality Standards of China (75 μg m^{-3} for 24 h average) (Sun et al., 2013). Aerosol particles have a large impact on visibility by scattering (Charlson et al., 1987; Tegen et al., 2000) and absorbing (Ramanathan and Vogelmann, 1997; Jacobson, 2001) solar and infrared radiation. The hygroscopic growth of aerosol particles will further increase their effect on atmospheric visibility (Quan et al., 2011). Therefore, haze events (with visibility < 10 km) appear frequently in Beijing, especially under high relative humidity (RH). However, the air pollution control

* Corresponding author. Beijing Weather Modification Office, Beijing, China.
** Corresponding author. National Center for Atmospheric Research, Boulder, CO, USA.
E-mail addresses: quanjn1975@gmail.com (J. Quan), xxtie@ucar.edu (X. Tie).

1352-2310/$ – see front matter © 2014 Elsevier Ltd. All rights reserved.
http://dx.doi.org/10.1016/j.atmosenv.2014.01.058

remains a great challenge due to the complex sources and evolution processes of aerosol particles, together with complicated aerosol-radiation-Planetary Boundary Layer (PBL) interactions.

In the last decade, extensive efforts have been made to characterize the sources, properties and processes of PM in Beijing. Recent studies indicate that a large mass fraction of ambient PM in Beijing is fine particles, of which carbonaceous particles, sulfate, nitrate and ammonium are the major components (Guinot et al., 2007; He et al., 2001; Yang et al., 2011). The secondary formation of coal/biomass burning products, crust, industrial and traffic emissions were the major sources of the fine aerosols in Beijing (Wang et al., 2005; Sun et al., 2010). The physical and chemical characteristics of aerosol particles affect directly their hygroscopic properties (Topping et al., 2005a,b). Liu et al. (2011) analyzed the hygroscopic growth factor at different RH for particles with dry diameters between 50 and 250 nm in North China Plain (NCP). Quan et al. (2011) calculated the visibility based on observed aerosol size distribution and their hygroscopic. Their results indicated that the calculated visibility with the hygroscopic growth of aerosol is consistent with measured visibility.

Moreover, the complicated aerosol-radiation-PBL interactions might further increase ground aerosol particles concentration and decrease visibility. The study of Quan et al. (2013) indicated that there might exist feedback between PBL height and aerosol loading. The enhancement of aerosols tends to depress the development of PBL by decreasing solar radiation, while the repressed structure of PBL will in turn weaken the diffusion of pollutants, leading to the heavy pollution. As a result, this possible positive feedback loop (more aerosols → lower PBL height → more aerosols) may induce an acceleration process for heavy ground pollution.

In this work, a comprehensive measurement was carried out in Beijing to understand the cause of haze events. The measured variables include some important meteorological parameters, such wind, RH, PBL, solar radiation, and visibility. The important aerosol composition and concentrations (including $PM_{2.5}$, NO_3, SO_4, NH_4, organic aerosol (OA), and chloride (Chl)) as well as their gas-phase precursors, including NO_x and SO_2 were measured. The analysis focus on the following issues: (a) characteristics of PBL, $PM_{2.5}$, solar radiation, RH, wind in haze events; and (b) the gas to particle conversions under low photochemical conditions.

2. Methods and instruments

2.1. Sampling site

This observation was conducted from Nov. 16, 2012 to Jan. 15, 2013 at Baolian (BL) meteorological station, Chinese Meteorological Administration (CMA) (39°56′N, 116°17′E), which is located between the west 3rd and 4th highways in Beijing. The distance of the station from nearby major roads is about 400 m. The surrounding region of this site is mainly residential district, without large point sources of $PM_{2.5}$. In this measurement, atmospheric visibility, mass concentration of $PM_{2.5}$, chemical composition of PM_1 (particle matter with the radius equal/less 1.0 μm), gaseous pollutants (SO_2, NO_x, CO, O_3), PBL heights were observed simultaneously, together with meteorology variables of temperature, RH, pressure, wind speed, and wind direction.

2.2. Instruments and observation

The mass concentration of $PM_{2.5}$ was observed by a R&P model 1400a Tapered Element Oscillating Microbalance (TEOM, Thermo Scientific Co., USA) instrument, with a 2.5 mm cyclone inlet and an inlet humidity control system. A dedicated sampling line was used to obtain 5-min averaged fine particulate mass concentrations. This instrument was installed in an air-conditioned room and was operated with a hydrophobic filter material to reduce the humidity of the incoming sampled air. The sample stream was preheated before entering the mass transducer. Thus semi-volatiles and water were not measured. The filter loading percentage and flow rates of TEOM were checked once a week, and the filter was replaced when the filter loading percentage was greater than 30% (see also Zhao et al., 2009).

Chemical composition of PM_1 was measured by an Aerodyne High-Resolution Time-of-Flight Aerosol Mass Spectrometer (HR-ToF-AMS). The details description of HR-ToF-AMS and its operation had been presented in many previous publications and reviewed by Drewnick et al. (2005). In the AMS, an aerodynamic lens was used to sample and focus ambient particles into a narrow beam that was transmitted to a heated surface (~600 °C), where particles were flashly vaporized. The resulting vapor molecules are ionized by 70 eV electron impaction (EI), and then the positive ions were analyzed by a ToF mass spectrometer. Because the aerodynamic lens has reduced transmission efficiencies for particles at sizes of approximately 1 μm and only non-refractory (NR) species (i.e., ammonium, sulfate, nitrate, chloride and organics) evaporate at the vaporizer temperature (~600 °C). As a result, the AMS measurements only represent non-refractory PM_1 (NR-PM_1). Particle size information was obtained by measuring particle velocity with a mechanical chopper wheel. The instrument provides 5 min averaged quantitative mass loading information on non-refractory components using a well characterized series of calibrations and error estimations (Jimenez et al., 2003; Allan et al., 2003, 2004), as well as species resolved size distributions. The HR-ToF-AMS calibration, e.g. inlet flow, ionization efficiency (IE) and particle sizing, was performed at the beginning, the middle and the end of the measurement period as the standard protocols recommend (Jayne et al., 2000; Jimenez et al., 2003; Drewnick et al., 2005).

A micro-pulse lidar (MPL-4B, Sigmaspace Co., USA) was employed to study the evolution of PBL. The PRF (pulse repetition frequency) of the MPL is 2500 Hz, with a wavelength of 532 nm of the laser beam. The peak value of the optical energy of laser beam is 8 μJ. The pulse duration was set to 100 ns, and the pulse interval was set to 200 ns, corresponding to a spatial resolution of 30 m. The PBL height is determined at the altitude where a sudden decrease in the scattering coefficient occurs (Boers and Eloranta, 1986; Brooks, 2003; Cohn and Angevine, 2000). The fundamental premise takes advantage of the large gradient in aerosol concentration that is generally evident between the boundary layer aerosols and those found in the free troposphere.

The concentrations of NO, NO_2, and NO_x = (NO + NO_2) were measured with a chemiluminescent trace level analyzer (TEI; Model 42iTL). The analyzer has a detection limit of 0.025 ppbv. The concentrations of CO were measured by the Model 48iTL enhanced CO analyzer, using a gas filter correlation technology, with a detection limit of 0.04 ppmv. SO_2 was detected with a pulsed UV fluorescence analyzer (TEI; Model 43 i-TLE). The detection limit for this analyzer is 0.05 ppbv for 2-min integration with a precision of about 0.20 ppbv. O_3 was measured with a UV photometric analyzer (Model 49iTL, TEI Inc.), with a detectable limit of 0.05 ppbv.

Atmospheric visibility was observed by a PWD20 (Vaisala Co., Finland), with range of 10–20,000 m, and meteorology variables were observed by WXT-510 (Vaisala Co., Finland).

3. Result and analysis

3.1. General characteristics of the haze events

Fig. 1 shows the measured variations of visibility, $PM_{2.5}$, PM_1, PBL heights, RH, and wind speeds during the 2012–2013 winter (from Nov. 17, 2012 to Jan. 15, 2013). The results indicate that the visibility

varied from a few hundred meters to more than 20 km. The haze events are defined by the visibility being less than 10 km in China, and there were frequent haze events occurred during the 2012–2013 winter. For example, from Dec. 11 to Dec. 16, 2012, the visibility was rapidly decreased, reaching to a minimum of 667 m on Dec. 16, 2012. During the haze occurrences, the concentrations of aerosols and RH were rapidly increased. The concentrations of $PM_{2.5}$ often exceeded 200 μg/m^3, with a maximum concentration of 600 μg/m^3 on Jan. 13, 2013. The RH was also increased during the haze events, indicating that both aerosol concentrations and RH had strong effect on the reduction of visibility, causing the occurrence of the haze events. Another important aspect is that the wind speeds were generally low during the 2012–2013 winter, with the wind speeds being smaller than 5 m/s. Moreover, during the haze events, the wind speeds were often less than 1 m/s, suggesting that the horizontal transport of aerosols was very weak, and vertical diffusion (including the PBL heights and the mixing of air pollutants in PBL) was an important process in controlling the variability of the surface concentrations of aerosols. As a result, the low PBL height was the major reason for the occurrences of the haze events (Quan et al., 2013). For example, the PBL height was about 1.5 km on Dec. 18 (with $PM_{2.5}$ of 50 μg/m^3), and quickly reduced to about 0.5 km on Dec. 23, 2012 (with $PM_{2.5}$ of 150 μg/m^3). The low layer of PBL compressed the aerosol particles into a shallow vertical layer, and prevented the vertical dispersion of the aerosol particles, leading to an increase in the surface aerosol concentrations, which is consistent to the previous study in the region (Zhang et al., 2009).

The growth of the PBL height is strongly depended on the surface solar radiation. With high solar radiation, PBL is fully developed, reaching a maximum of the PBL heights in the noontime. However, if solar radiation is absorbed or scattered by aerosol particles or cloud layers, the PBL cannot be fully developed, and the daytime PBL heights could be significantly reduced (Yu et al., 2002). Fig. 2 illustrates that during the haze events, the surface solar radiation was reduced, while the surface scattering of solar radiation was increased, leading to the decrease in the PBL heights. This result demonstrated that aerosol particles (especially the scattering particles, such as SO_4, NO_3, and organic carbon (OC)) play important roles for reducing the development of PBL heights during the daytime. Further more, the lower PBL height depresses the aerosol particles, leading to the increase of aerosol concentrations and causing further decrease in the solar radiation and the PBL heights, which induces a positive feedback loop for causing high surface aerosol concentrations (Quan et al., 2013).

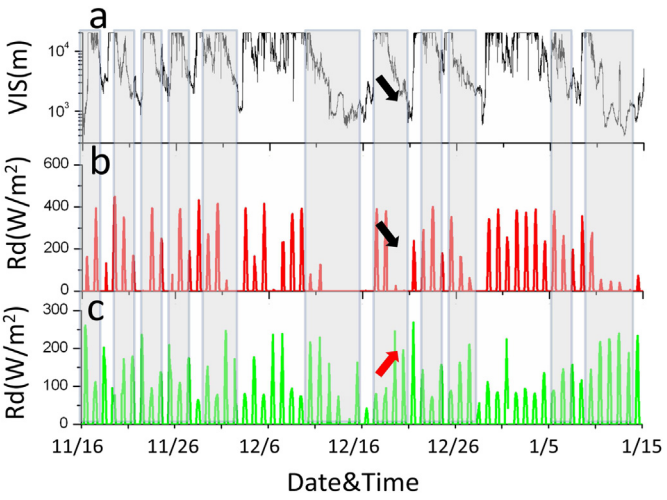

Fig. 2. Time series of visibility (a, same as in Fig. 1a), direct solar radiation measured by TBS-2-B (Huatron CO., China) with spectrum of 0.3–3 μm (see panel b), and scattered radiation measured by TBQ-2-B (Huatron CO., China) with spectrum of 0.3–3 μm (see panel c).

3.2. Variations of aerosol particles and precursors

In order to get more insights of the heavy aerosol pollution in the period, detailed aerosol composition and the gas-phase precursors were analyzed. Fig. 3 shows the diurnal variations of aerosol precursors, including SO_2, NO_x, CO, and O_3, and the various aerosol

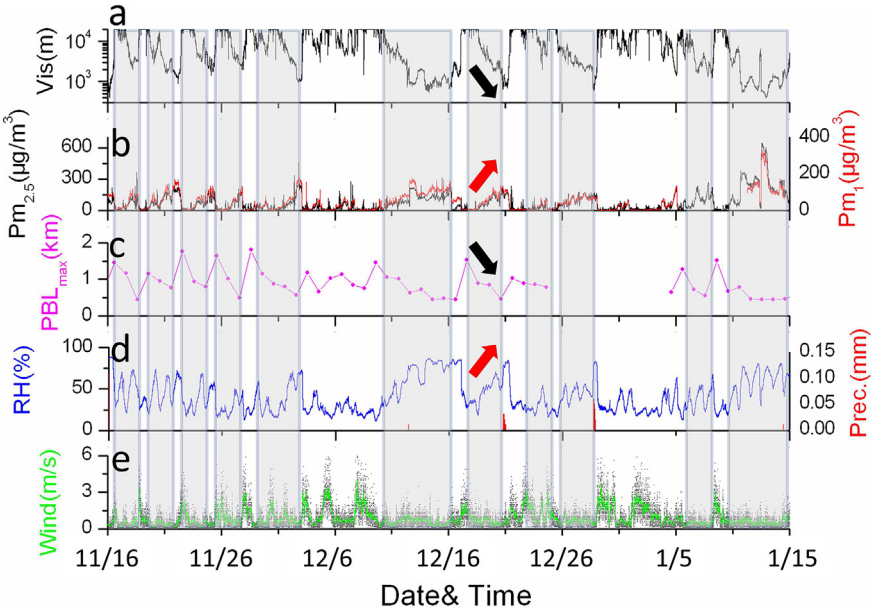

Fig. 1. Time series of visibility measured by PWD20 with time resolution of 1 min (a), $PM_{2.5}$ measured by TEOM (black line) and NR-PM_1 measured by HR-ToF-AMS (red line) with time resolution of 5 min (b), daily averaged PBL height between 13:00 and 15:00 measured by MPL (c), RH (blue line) with time resolution of 1 min and precipitation (red line) with time resolution of 1 h (d), and wind speed with time resolution of 1 min (black dot) and 1 h (green line) (e). (For interpretation of the references to color in this figure legend, the reader is referred to the web version of this article.)

compounds, including NO_3, SO_4, NH_4, Chl, secondary organic carbon (SOA), primary organic carbon (POA), and $PM_{2.5}$ under three different visibility conditions (i.e., (1) all data, (2) visibility < 5 km, and (3) visibility ≥ 5 km). For the gas-phase compounds (SO_2, CO, NO_x, and O_3), the diurnal variations were very different between the species which are mainly due to direct surface emissions (SO_2, CO, and NO_x) and the species which are mainly controlled by the photochemical process (such as O_3). For example, the NO_x concentrations were high in the morning, and quickly reduced in the noontime due to the strong elevation of the PBL heights, suggesting the important impacts of the PBL heights on the surface NO_x concentrations, which is consistent to previous study (Tie et al., 2007). However, for O_3 concentrations, during the noontime, the concentrations reached a maximum when the PBL is high. This is because of the strong photochemistry during the noontime. This result suggested that the chemical species, which are strongly controlled by the photochemical process, are weakly regulated by the development of the PBL, while the chemical species, which are mainly produced by the surface emissions, are strongly controlled by the development of the PBL heights. This conclusion is also applied to the diurnal variation of aerosol particles. For example, POA and Chl are mainly produced by the surface emissions. Much of the Chloride in the atmosphere comes from coal combustion (McCulloch et al., 1999). In China, coal is the dominant energy resources. Therefore the proportion of chloride in aerosol is very high in China, especially during heating period in winter (Sun et al., 2012, 2013). As a result, there was a clearly minimum at the noontime. However, for the secondary aerosol particles (NO_3, SO_4, NH_4, and SOA), which are mainly produced by the chemical processes, there was a maximum in the late afternoon.

Fig. 3 also suggests that both gas-phase compounds and aerosol particles had different characteristics in the different visibility levels. The differences were mostly for the magnitudes of concentrations, while the diurnal variation had a similar pattern. For example, under the low visible condition, the $PM_{2.5}$ concentrations were generally greater than 100 μg/m^3, while under the high visibility condition, the $PM_{2.5}$ concentrations were less than 50 μg/m^3. It is interesting to note that the levels of O_3 concentrations were very sensitive to the visibility levels. Under the low visibility condition, the ozone photochemical production was almost ceased, and the maximum O_3 concentration was only a few ppb. Because the formation of SO_4 and NH_4 has important impact on the visibility, the O_3 reduction is also associated with the chemical conversions of SO_2 and NO_3 to SO_4 and NH_4.

The ratios between aerosol particles of nitrogen and sulfate (N_a and S_a) and the total nitrogen and sulfur (both gas and particle phase; $N_a + N_g$ and $S_a + S_g$) are analyzed (shown in Fig. 3). During the low visibility condition, the ratios were increased, especially for the ratio of sulfate. This result suggests that during the heavy haze condition (with a low photochemical activity), there was a rapid chemical conversion from gas phase to particle phase for nitrate and sulfate, especially for sulfate particles. Because the particles were produced under very low photochemical activity (e.g., O_3 production was extremely low), the conversion of the particles was mainly produced through the processes other than the photochemical activities (such as heterogeneous conversions). This result is consistent with a recent study that sulfate particles were rapidly formed under the heavy fog conditions in the Beijing region (Zhang et al., 2013).

3.3. Conversion from gas to particle phases

In order to get more detailed analyses of the conversion from the aerosol precursors to aerosol particles, three different visibility conditions are defined, i.e., V1 (VIS $\geq$ 5 km), V2 (2 km $\leq$ VIS $<$ 5 km), and V3 (VIS $<$ 2 km). Fig. 4 shows the relationship between CO and NO_x under the three conditions. It shows that the concentrations of NO_x were continuously reduced when the visibility were decreased, indicating more evidences that the conversion from gas to particles was enhanced under the low visibility condition. For example, with CO concentration of 4 ppm, the corresponding NO_x concentration was very high (about 70 ppbv)

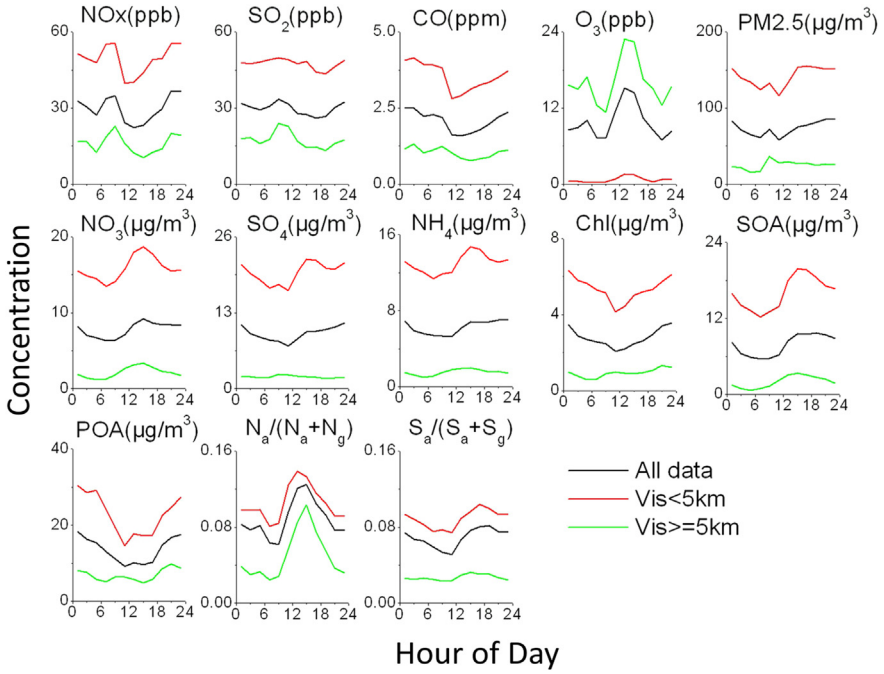

Fig. 3. Diurnal profiles of aerosol precursors (NO_x, SO_2, CO, O_3), $PM_{2.5}$, and various aerosol compounds measured by AMS (NO_3, SO_4, NH_4, Chl, POA, and SOA), and the mole ratios of particle phase of nitrogen and sulfate (N_a and S_a) to total nitrogen and sulfate (both gas and particle phase; $N_a + N_g$ and $S_a + S_g$).

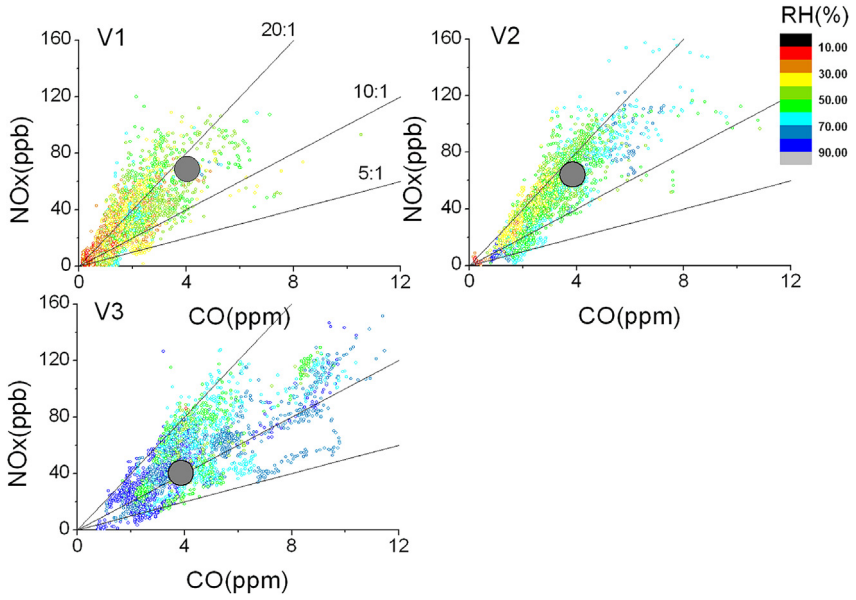

Fig. 4. Relationship between NO_x and CO under different visibility conditions. The three conditions are classified as: VIS ≥5 km (V1), 2 km ≤ VIS < 5 km (V2), and VIS < 2 km (V3).

under the V1 condition. Under the V2 condition, the haze was medium, and the NO_x concentration was decreased to about 60 ppbv. With further decrease in visibility and the high haze condition (the V3 condition), the NO_x concentration reduced to about 40 ppbv. The slopes between CO and NO_x concentrations (the ratios between CO and NO_x) were about 17.5, 15, and 10 ppbv/ppmv under V1, V2, and V3, respectively. The same situation also occurred in the CO–SO_2 correlation (shown in Fig. 5). With CO concentration of 4 ppm, the corresponding SO_2 concentrations varied from 70, 50, and 40 ppbv, with the slopes between CO and SO_2 concentrations being 17.5, 12.5, and 10 ppbv/ppmv under V1, V2, and V3, respectively. One of the reasons to explain the enhancement of in the slopes of $\Delta NO_x/\Delta CO$ and $\Delta SO_2/\Delta CO$ under low visibility (low photochemical) condition is that there were heterogeneous conversions from gas to particle phases for resulting in the reductions of NO_x and SO_2.

According to the above analysis, the aerosol precursors were reduced under the low photochemical condition due to the conversion of gases → particles. To further verify this result, the aerosol particle formation under the different visibility conditions was studied. Fig. 6 shows the percentage of different aerosols (organic carbon-ORG, NO_3, SO_4, NH_4, and Chl) under the different visibility conditions. Because the limitation of AMS, black carbon and dust particles are not included in the analysis. There was a clear difference of the aerosol composition with the changes in the visibility conditions. For example, with high visibility (VIS ≥ 5 km), the averaged aerosol concentration was low (15.4 μg/m^3). The percentage of ORG was the highest (57%), following by NO_3 (14%), SO_4 (13%), NH_4 (10%), and Chl (6%). Under the medium condition (2 km < VIS < 5 km), the averaged aerosol concentration increased to 67.7 μg/m^3. The percentage of ORG was still the highest, but decreased from 57% to 50%. In contrast, the percentages of

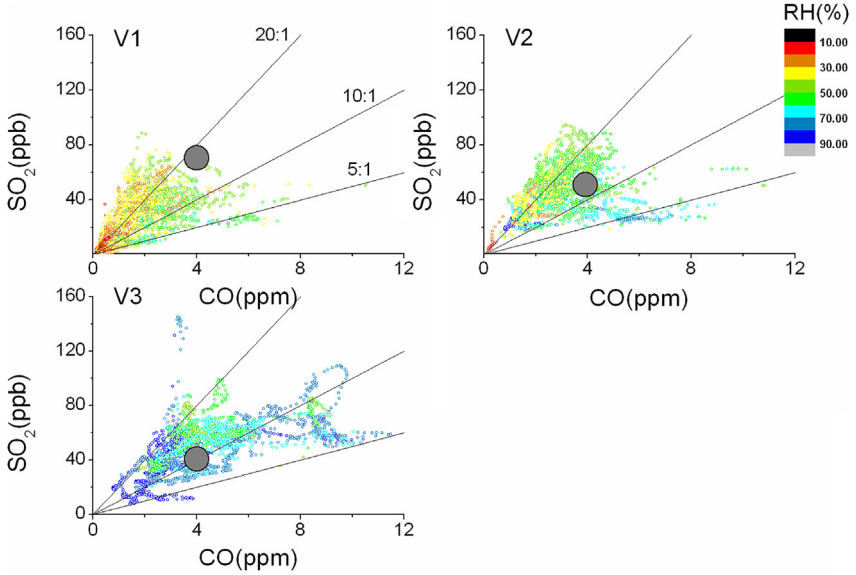

Fig. 5. Relationship between SO_2 and CO under different visibility conditions. The three conditions are classified as in Fig. 4.

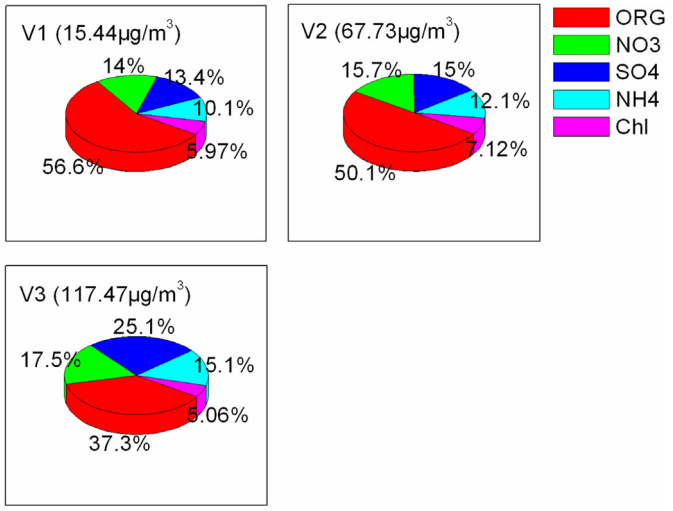

Fig. 6. Aerosol composition measured by AMS under different visibility conditions. The three conditions are classified as in Fig. 4.

secondary aerosol particles (NO_3, SO_4, and NH_4) increased. For example, NO_3 changed from 14% to 16%; SO_4 changed from 13% to 15%; and NH_4 increased from 10% to 12%. Under the extremely low visibility condition (VIS $<$ 2 km), the averaged aerosol concentration reached to highest value of 117.5 μg/m^3. The percentage of ORG further decreased to 37%, and the percentages of NO_3 increased to 17%, SO_4 increased to 25%, and NH_4 increased to 15%. This analysis suggests that the particle formation, especially nitrate and sulfate, was enhanced under "dark" (low photochemical) condition. Fig. 7 shows that the ratios of particle phases of nitrate and sulfate were strongly dependent upon the visibility ranges, especially the sulfate particles. The nitrate and sulfate formation were about 2 and 5 times higher under the V3 condition than the V1 condition.

Combining with the changes in aerosol precursors (NO_x and SO_2), this result suggested that the conversion between the gas precursors and particles was enhanced during the lower visibility condition (higher haze and lower photochemical conditions), indicating a significant heterogeneous formation for nitrate and sulfate particles during the heavy haze events.

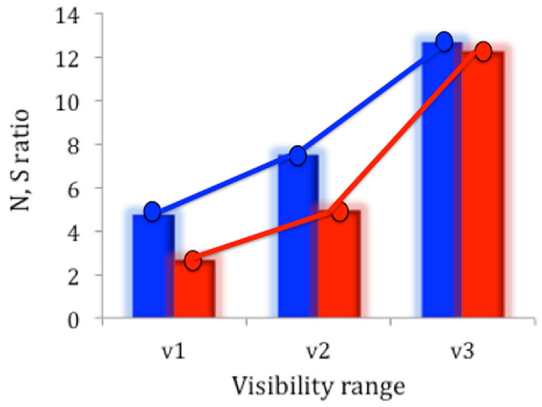

Fig. 7. Mol ratios of particle phase of nitrogen (blue) and sulfate (red) (N_a and S_a) in total nitrogen and sulfate (both gas and particle phase; $N_a + N_g$ and $S_a + S_g$) under different visibility conditions. The three conditions are classified as in Fig. 4. (For interpretation of the references to color in this figure legend, the reader is referred to the web version of this article.)

4. Summary

A comprehensive measurement was made to study the heavy haze event during 2012–2013 winter in Beijing. The results are highlighted as follows:

(1) During the haze occurrences, the hourly mean concentrations of $PM_{2.5}$ often exceeded 100 μg/m^3, with a maximum concentration of 600 μg/m^3 on Jan. 13, 2013. The RH was also increased during the haze events, indicating that both aerosol concentrations and RH had strong effect for the reduction of visibility, causing the occurrence of the haze events.

(2) The wind speeds were generally low (less than 1 m/s) during the haze event. As a result, the vertical dispersion played an important role in controlling the aerosol variability. The result shows that PBL height was about 1.5 km on Dec. 18, 2012 (with $PM_{2.5}$ of 50 μg/m^3), and quickly reduced to about 0.5 km on Dec. 23, 2013 (with $PM_{2.5}$ of 150 μg/m^3). The lower PBL height compressed the aerosol particles into a shallow layer, and prevented the vertical dispersion of the aerosol particles, leading to an increase in the surface aerosol concentrations.

(3) Under different visibility conditions, i.e., V1 (VIS $\geq$ 5 km), V2 (2 km $\leq$ VIS $<$ 5 km), and V3 (VIS $<$ 2 km), the slopes of $\Delta NO_x/\Delta CO$ and $\Delta SO_2/\Delta CO$ were changed. For example, the slopes of $\Delta NO_x/\Delta CO$ were 17.5, 15, and 10 ppbv/ppmv, and the slopes of $\Delta SO_2/\Delta CO$ were 17.5, 12.5, and 10 ppbv/ppmv under V1, V2, and V3, respectively. This result suggests that more gas phase of NO_x and SO_2 were converted to the particle phase under the lower visibility condition. As a result, the particle phase of NO_3 and SO_4 was higher in the lower visibility condition (V1) than in the higher visibility condition (V3). For example, under the V1 condition, the percentage of NO_3 and SO_4 were 14 and 13%. In contrast, the percentage of NO_3 and SO_4 were 17 and 25% under the V3 condition. Because under the lower visibility condition, the photochemical conversion from gas to particle phase should be lower, the higher conversion indicated that there were higher heterogeneous conversions from gas to particle phases of NO_x and SO_2 during the heavy haze events.

Acknowledgments

This research is partially supported by National Basic Research Program of China (2011CB403401). This research is also partially supported by National Natural Science Foundation of China (NSFC) under Grants No. 41275168 and 41175007, and the Projects of Beijing Municipal Science & Technology Commission under Grant No. Z131100005613024, 2010B029, Z131109002813038. The National Center for Atmospheric Research is sponsored by the National Science Foundation.

References

Allan, J.D., Jimenez, J.L., Coe, H., Bower, K.N., Williams, P.I., Worsnop, D.R., 2003. Quantitative sampling using an aerodyne aerosol mass spectrometer. Part 1: techniques of data interpretation and error analysis. Journal of Geophysical Research 108, 4090. http://dx.doi.org/10.1029/2002JD002358.

Allan, J.D., Coe, H., Bower, K.N., Alfarra, M.R., Delia, A.E., Jimenez, J.L., Middlebrook, A.M., Drewnick, F., Onasch, T.B., Canagaratna, M.R., Jayne, J.T., Worsnop, D.R., 2004. Technical note: extraction of chemically resolved mass spectra from aerodyne aerosol mass spectrometer data. Journal of Aerosol Science 35, 909–922.

Boers, R., Eloranta, E.W., 1986. Lidar measurements of the atmospheric entrainment zone and the potential temperature jump across the top of the mixed layer. Boundary-Layer Meteorology 34, 357–375.

Brooks, I.M., 2003. Finding boundary layer top: application of a wavelet covariance transform to lidar backscatter profiles. Journal of Atmospheric and Oceanic Technology 20, 1092–1105.
Chan, C.K., Yao, X., 2008. Air pollution in megacities in China. Atmospheric Environment 42 (1), 1–42.
Charlson, R.J., Lovelock, J.E., Andreae, M.O., Warren, S.G., 1987. Oceanic phytoplankton, atmospheric sulfur, cloud albedo and climate. Nature 326, 655–661.
Cohn, S.A., Angevine, W.M., 2000. Boundary layer height and entrainment zone thickness measured by lidars and wind-profiling radars. Journal of Applied Meteorology 39, 1233–1247.
Drewnick, F., Hings, S.S., DeCarlo, P., Jayne, J.T., Gonin, M., Fuhrer, K., Weimer, S., Jimenez, J.L., Demerjian, K.L., Borrmann, S., Worsnop, D.R., 2005. A new Time-of-Flight Aerosol Mass Spectrometer (TOF-AMS)-instrument description and first field deployment. Aerosol Science and Technology 39, 637–658.
Guinot, B., Cachier, H., Sciare, J., Yu, T., Wang, X., Yu, J.H., 2007. Beijing aerosol: atmospheric interactions and new trends. Journal of Geophysical Research 112 (D14314). http://dx.doi.org/10.1029/2006JD008195.
He, K.B., Yang, F., Ma, Y.L., Zhang, Q., Yao, X.H., Chan, C.K., Cadle, S., Chan, T., Mulawa, P., 2001. The characteristics of $PM_{2.5}$ in Beijing, China. Atmospheric Environment 35, 4959–4970.
Jacobson, M.Z., 2001. Strong radiative heating due to the mixing state of black carbon in atmospheric aerosols. Nature 409, 695–697.
Jayne, J.T., Leard, D.C., Zhang, X., Davidovits, P., Smith, K.A., Kolb, C.E., Worsnop, D.R., 2000. Development of an aerosol mass spectrometer for size and composition, analysis of submicron particles. Aerosol Science and Technology 33, 49–70.
Jimenez, J.L., Jayne, J.T., Shi, Q., Kolb, C.E., Worsnop, D.R., Yourshaw, I., Seinfeld, J.H., Flagan, R.C., Zhang, X., Smith, K.A., Morris, J.W., Davidovits, P., 2003. Ambient aerosol sampling using the aerodyne aerosol mass spectrometer. Journal of Geophysical Research 108, 8425. http://dx.doi.org/10.1029/2001JD001213.
Liu, P.F., Zhao, C.S., Gobel, T., Hallbauer, E., Nowak, A., Ran, L., Xu, W.Y., Deng, Z.Z., Ma, N., Mildenberger, K., Henning, S., Stratmann, F., Wiedensohler, A., 2011. Hygroscopic properties of aerosol particles at high relative humidity and their diurnal variations in the North China Plain. Atmospheric Chemistry and Physics 11, 3479–3494.
McCulloch, A., Aucott, M.L., Benkovitz, C.M., Graedel, T.E., Kleiman, G., Midgley, P.M., Li, Y.F., 1999. Global emissions of hydrogen chloride and chloromethane from coal combustion, incineration and industrial activities: reactive chlorine emissions inventory. Journal of Geophysical Research 104, 8391–8403.
Quan, J.N., Gao, Y., Zhang, Q., Tie, X.X., Cao, J., Han, S., Meng, J., Chen, P., Zhao, D., 2013. Evolution of planetary boundary layer under different weather conditions, and its impact on aerosol concentrations. Particuology 11, 34–40.
Quan, J.N., Zhang, Q., Liu, J.Z., Huang, M.Y., Jin, H., 2011. Analysis of the formation of fog and haze in North China Plain (NCP). Atmospheric Chemistry and Physics 11, 8205–8214.
Ramanathan, V., Vogelmann, A.M., 1997. Greenhouse effect, atmospheric solar absorption, and the Earth's radiation budget: from the Arrhenius–Lanely era to the 1990s. Ambio 26 (1), 38–46.
Sun, J., Zhang, Q., Canagaratna, M.R., Zhang, Y., Ng, N.L., Sun, Y., Jayne, J.T., Zhang, X., Zhang, X., Worsnop, D.R., 2010. Highly time- and size-resolved characterization of submicron aerosol particles in Beijing using an Aerodyne Aerosol Mass Spectrometer. Atmospheric Environment 44, 131–140.
Sun, Y.L., Wang, Z.F., Dong, H.B., Yang, T., Li, J., Pan, X.L., Chen, P., Jayne, J.T., 2012. Characterization of summer organic and inorganic aerosols in Beijing, China with an Aerosol Chemical Speciation Monitor. Atmospheric Environment 51, 250–259.
Sun, Y.L., Wang, Z.F., Fu, P.Q., Yang, T., Jiang, Q., Dong, H.B., Li, J., Jia, J.J., 2013. Aerosol composition, sources and processes during wintertime in Beijing, China. Atmospheric Chemistry and Physics 13, 4577–4592.
Tegen, I., Koch, D., Lacis, A.A., Sato, M., 2000. Trends in tropospheric aerosol loads and corresponding impact on direct radiative forcing between 1950 and 1990: a model study. Journal of Geophysical Research 105, 26971–26990.
Tie, X., Madronich, S., Li, G.H., Ying, Z.M., Zhang, R., Garcia, A., Lee-Taylor, J., Liu, Y., 2007. Characterizations of chemical oxidants in Mexico City: a regional chemical/dynamical model (WRF-Chem) study. Atmospheric Environment 41, 1989–2008.
Topping, D.O., McFiggans, G.B., Coe, H., 2005a. A curved multi-component aerosol hygroscopicity model framework: part 1-inorganic compounds. Atmospheric Chemistry and Physics 5, 1205–1222.
Topping, D.O., McFiggans, G.B., Coe, H., 2005b. A curved multicomponent aerosol hygroscopicity model framework: part 2 – including organic compounds. Atmospheric Chemistry and Physics 5, 1223–1242.
Wang, Y., Zhuang, G., Tang, A., Yuan, H., Sun, Y., Chen, S., Zheng, A., 2005. The ion chemistry and the source of $PM_{2.5}$ aerosol in Beijing. Atmospheric Environment 39, 3771–3784.
Yang, F., Tan, J., Zhao, Q., Du, Z., He, K., Ma, Y., Duan, F., Chen, G., 2011. Characteristics of $PM_{2.5}$ speciation in representative megacities and across China. Atmospheric Chemistry and Physics 11, 5207–5219.
Yu, H., Liu, S.C., Dickinson, R.E., 2002. Radiative effects of aerosols on the evolution of the atmospheric boundary layer. Journal of Geophysical Research 107, 4142. http://dx.doi.org/10.1029/2001JD000754.
Zhang, Q., Ma, X., Tie, X., Huang, M., Zhao, C., 2009. Vertical distributions of aerosols under different weather conditions: analysis of in situ aircraft measurements in Beijing China. Atmospheric Environment 43, 5526–5535.
Zhang, Q., Tie, X., Lin, W., Cao, J., Quan, J., Ran, L., Xu, W., 2013. Measured variability of SO_2 in an intensive fog event in the NCP region, China; evidence of high solubility of SO_2. Particuology 11, 41–47.
Zhao, X.J., Zhang, X.L., Xu, X.F., Xu, J., Meng, W., Pu, W., 2009. Seasonal and diurnal variations of ambient $PM_{2.5}$ concentration in urban and rural environments in Beijing. Atmospheric Environment 43, 2893–2900.